Iranian Journal of Chemical Engineering
Vol. 16, No. 2 (Spring 2019), IAChE

The CFD Providing Data for Adaptive Neuro-Fuzzy to Model the Heat Transfer in Flat and Discontinuous Fins

R. Beigzadeh [*]

Department of Chemical Engineering, Faculty of Engineering, University of Kurdistan, Sanandaj, Iran

ARTICLE INFO

Article history:
Received: 2018-09-12
Accepted: 2019-04-08

Keywords:
Flat and Discontinuous Fin,
Heat Transfer,
Pressure Drop,
Computational Fluid Dynamic (CFD),
Adaptive Neuro–Fuzzy Inference System (ANFIS)

ABSTRACT

In the present study, Adaptive Neuro-Fuzzy Inference System (ANFIS) approach was applied for predicting the heat transfer and air flow pressure drop on flat and discontinuous fins. The heat transfer and friction characteristics were experimentally investigated in four flat and discontinuous fins with different geometric parameters including fin length (r), fin interruption (s), fin pitch (p), and fin thickness (t). Two ANFIS models were developed using the Computational Fluid Dynamic (CFD) results, as validated by the experimental data. The ANFIS models were applied for prediction of Nusselt number (Nu) and friction factor (f) as functions of Reynolds number (Re) and fin geometric parameters including span-wise spacing ratio (p/t) and stream wise spacing ratio (s/r). The low error values for testing data set, which were not employed in the training of the ANFIS, proved the precision and validity of the model. The root mean square error (RMSE) of 0.7343 and mean relative error (MRE) of 1.33 % were obtained for Nu prediction. In addition, these values for the estimation of f were obtained as 0.0158, 3.32 %, respectively.

1. Introduction

The advantages of the fins such as the large heat transfer area and high thermal performance have led to a great deal of research. The numerical and experimental studies of thermal and fluid flow characteristics of the various fins such as plain [1–3], pin [4–6], offset strip [7, 8], wavy [9, 10], and perforated [11] have been performed in the literature. Due to the influence of the fins geometric parameters on thermal-hydraulic performance, it is very useful to propose accurate numerical models for predicting heat transfer and flow characteristics. The accurate and reliable predictive models can be used for designing and optimizing the thermal systems.

The CFD analysis of the effects of the plain and pin fin geometries was performed by Diani et al. [2]. The investigated geometrical parameters include fin height, fin thickness, and fin pitch. The model validation was confirmed by the experimental measurements of a reference trapezoidal finned surface. Mon and Gross [12] numerically investigated the influence of fin spacing in annular-finned tube bundles for staggered and in-line arrangements on thermal performance. The

[*]Corresponding author: r.beigzadeh@uok.ac.ir

research results indicated that the fin spacing and Reynolds number influenced the development of the boundary layers. Rao et al. [4] experimentally and numerically investigated the thermal-hydraulic behavior of pin fin-dimple and pin fin channels. The heat transfer coefficients and flow pressure drop of the two cases were analyzed. The higher heat transfer coefficients around 8 % and lower friction characteristic around 18 % were obtained for a pin fin-dimple channel. The CFD modeling shows that the dimples increase the turbulent intensity close to the wall by producing strong vortex flows and cause the enhancement of heat transfer coefficient. A numerical investigation for optimizing the geometric parameters of the heat sinks with micro square pin fin was performed by Zhao et al. [6]. The optimized geometries of the micro square pin fins including fin porosity and fin located angle were presented for enhancing the cooling performance.

The Artificial Intelligence (AI) approaches including Artificial Neural Network (ANN), Adaptive Neuro-Fuzzy Inference System (ANFIS), and Genetic Algorithm (GA) are useful approaches for the modeling, prediction, and optimization of the thermal-hydraulic characteristics in thermal systems. Bar et al. [13] investigated the application of ANN modeling for predicting the frictional pressure drop in orifices, different valves, and elbows for non-Newtonian liquid flow. The application of ANN- and GA-based correlations to estimate thermal-hydraulic performance in serpentine microchannels was investigated by Rahimi et al. [14]. The results showed that the ANN could predict target data more accurate than the GA-based correlations. Momayez et al. [15] proposed correlations in the form of the classical power law for predicting the heat transfer characteristics for concave surfaces such as pressure side of the gas turbine blade. The constants of the developed correlations were obtained using the genetic algorithm approach.

The present study aims to investigate the ability of the ANFIS in predicting the thermal and fluid flow characteristics in flat and discontinuous fins. The heat transfer and pressure drop of the air flowing on surfaces equipped with interrupted rectangular fins were measured experimentally. The various geometry fins were applied to the experimental work. The CFD technique was applied to simulate the studied fins and, then, the numerical data were validated by the experimentally obtained results. For reducing the experimental effort, the valid numerical approach was used for providing the adequate numerical-validated data (CFD data) to develop ANFIS models. Two adaptive neuro-fuzzy models were trained for estimating the target data as functions of input values. In the research, target data include the Nusselt number (Nu) and friction factor (f); input data are fin geometrical parameters (p/t and s/r) and Reynolds number (Re).

2. Experimental setup

The experiments were performed in the experimental setup, as schematically illustrated in Fig. 1. The experimental facility consists of an adjustable speed blower, two pressure transducers, an air flow meter, temperature measuring devices, and a test section. The air flow speed driven into the wind tunnel was measured by means of the hot wire anemometer ST-8880.

The wind tunnel has a rectangular cross-section and includes three parts test channel (in the middle of the tunnel) with dimensions

of 30×40×500 mm and two channels in the entrance and output of the tunnel with dimensions of 80×80×250 mm. In order to provide a suitable thermal insulation, the channel walls were made of medium-density fibreboard with 1.6 cm thickness. Four fins with various geometries including fin length (r), fin interruption (s), fin pitch (p), and fin thickness (t) were investigated experimentally. Table 1 reports the details of the fin dimensions. A real photo of a flat and discontinuous fin (layout number 2) and its main geometrical parameters is shown in Fig. 2. For the aluminum fins, N is considered as the number of arrays in spanwise and M is the number of arrays in streamwise direction (see Table 1). The base of the fins was heated by a plate-type heater, which was linked to an AC power supply. Two thermocouples (K-type) with the accuracy of 0.05 K were used for measuring the fin base temperature. Two holes were drilled at the inlet and outlet of the fin base for inserting the thermocouples. The effect of the fluid flow rate was investigated by six blower rotation speeds. A cover plate was carefully installed above the fin arrays and was flushed with the bottom wall of the channel. Two pressure transducers were placed at the upstream and downstream of the plate fins measured the pressure drops. The temperatures of the inlet and outlet of the test channel were measured using two K-type thermocouples.

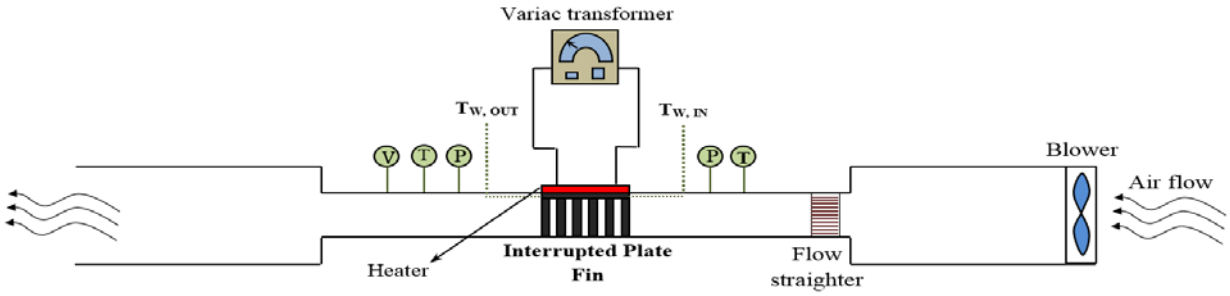

Figure 1. The experimental setup.

Table 1
Details of the fins used in the experiments (dimensions are in millimeters).

Layout number	N	M	W	L	H	t	p	s	r	b
1	7	6	37.7	41	26	1.1	6.1	7	6	1.5
2	8	4	36	38	20	1	5	10	8	3
3	9	8	37.5	38	22	1.5	4.5	5	3	2
4	10	6	35	40	27	1.1	3.7	7	5	3

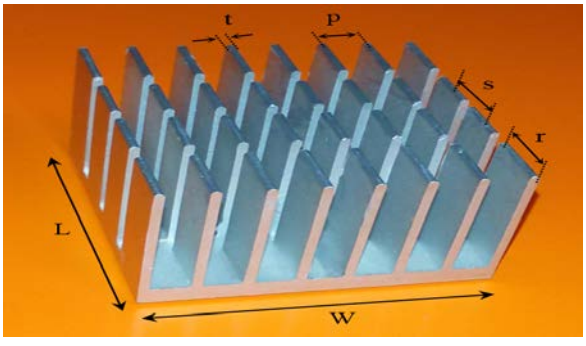

Figure 2. The flat and discontinuous fin (layout number 2) and main geometric parameters.

The imposed heat flux from the base of the heat sink to the air flow is calculated as follows:

$$Q = MC_{p.Air}(T_{Air,Out} - T_{Air,In}) \quad (1)$$

where M is the air mass flow rate, $C_{p,Air}$ is the specific heat capacity of air, $T_{Air,Out}$ and $T_{Air,In}$ are the outlet and inlet bulk temperatures of the air flow, respectively. The heat transfer rate to the fluid flow was obtained as follows:

$$Q = h A_{tot} \Delta T_{lm} \quad (2)$$

where h is the average heat transfer coefficient, and A_{tot} is the finned surface total area for the convective heat transfer. The logarithmic mean temperature difference between the wall and the working fluid can be found according to the following equation:

$$\Delta T_{lm} = \frac{(T_{W,Out} - T_{Air,Out}) - (T_{W,In} - T_{Air,In})}{\ln \frac{T_{W,Out} - T_{Air,Out}}{T_{W,In} - T_{Air,In}}} \quad (3)$$

in which $T_{W,Out}$ and $T_{W,In}$ are the temperatures at the outlet and inlet parts of the fin base, respectively. The heat transfer coefficients and the Nusselt numbers were obtained through the following relations:

$$h = \frac{MC_{p.Air}(T_{Air,Out} - T_{Air,In})}{A_{tot} \Delta T_{lm}} \quad (4)$$

$$Nu = \frac{hD_h}{k_{Air}} \quad (5)$$

where k_{Air} is the thermal conductivity of air, and D_h is the hydraulic diameter. The Reynolds number is calculated as follows:

$$\mathrm{Re} = \frac{\rho_{Air} u_{\max} D_h}{\mu_{Air}} \quad (6)$$

in which ρ_{Air} is the air density, μ_{Air} is the air dynamic viscosity, and u_{max} is the maximum velocity of the fluid occurring within the plate-fin array. The friction factor can be obtained according to the following relation:

$$f = \frac{2\Delta P D_h}{\rho_{Air} u_{\max}^2 L} \quad (7)$$

in which ΔP is the pressure drop across the flat and discontinuous fins, and L is the length of the plate fin. In this investigation, the uncertainty analysis of the reduced data was performed using the procedure presented by Holman [16]. The uncertainties about 3.8 %, 5.1 %, and 5 % were calculated for Re, Nu, and f, respectively.

3. Modeling study

The three-dimensional numerical modeling by means of the commercial CFD code, FLUENT, was used for simulating the experimentally investigated fins (reported in Table 1). The CFD modeling approach leads to an alternative for decreasing the experimental efforts. The CFD results were validated by the experimental data, which were previously obtained. After proving the validity of the model, the computational fluid dynamic technique was applied for modeling fins with different geometries. Table 2 lists the details of the dimensions of the flat and discontinuous fins, which were studied by the CFD technique. All fins are considered with the same similar dimensions such as a width of 40, a length of 40, a fin height of 20, and a base height of 2.5 mm.

Due to the symmetry of the investigated system, a single channel of the fined surfaces was simulated to decrease the computation effort. The computational domain and details of the boundary conditions are shown in Fig. 3. The three-dimensional geometries of the flat and discontinuous fins were created using

the commercial software GAMBIT 2.2. The computational fluid domain begins 20 mm (L/2) before the solid domain and extends 20 mm from the solid domain. The boundary conditions of the no-slip were employed for the interfaces of solid and fluid, as well as for top domain and bottom duct of the fluid domain at the input and output. The fluid domain inlet and outlets are treated as velocity-inlet (with a temperature of 25 °C) and pressure-outlet boundary conditions, respectively. The results indicate that, for more than approximately 400,000 tetrahedral cells, no more significant change occurs for the obtained values. The areas near the fluid and solid interface were meshed by finer meshes to achieve more precise estimation results. A typically mesh for the finned surface is shown in Fig. 3.

Table 2
Details of the flat and discontinuous fins used for modeling (dimensions are in millimeters).

Case number	*N*	*M*	*t*	*p*	*r*	*s*
1	5	5	1	8	3	9.25
2	5	5	2	8	3	9.25
3	5	5	3	8	3	9.25
4	5	5	4	8	3	9.25
5	6	6	1	6.67	3	7.4
6	6	6	2	6.67	3	7.4
7	6	6	3	6.67	3	7.4
8	6	6	4	6.67	3	7.4
9	7	7	1	5.71	3	6.17
10	7	7	2	5.71	3	6.17
11	7	7	3	5.71	3	6.17
12	7	7	4	5.71	3	6.17
13	8	8	1	5	3	5.29
14	8	8	2	5	3	5.29
15	8	8	3	5	3	5.29
16	8	8	4	5	3	5.29
17	7	7	2	5.71	2	6.33
18	7	7	2	5.71	4	6
19	7	7	2	5.71	5	5.83

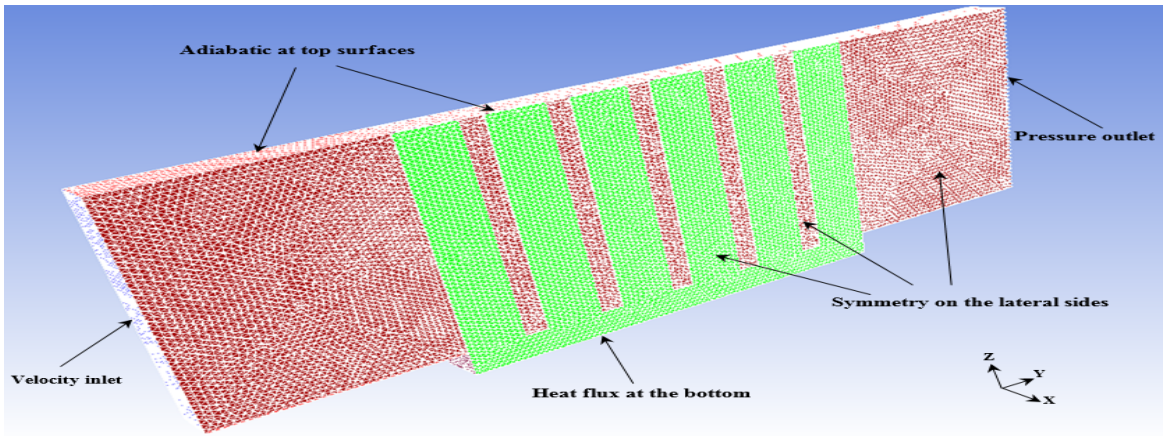

Figure 3. The numerical mesh of the flat and discontinuous fin and boundary conditions.

In the present work, the realizable k-ε turbulence model [17] was applied to model the turbulent regime in the flat and discontinuous fins. The model-related equations for the extended surfaces are presented in references [2, 4]. For the pressure–velocity coupling, the SIMPLE algorithm was selected and, for the momentum, energy, turbulent kinetic energy and dissipation energy, the second-order volume discretization scheme was used. The minimum convergence criterion was considered (10-4) for all calculation parameters, excluding the energy equation where (10-7) was employed.

3.1. ANFIS modeling

The ANN does not include explicit information or causal relation for a system, and it can be treated as a major drawback of the neural network [18]. The combination of neural network and fuzzy system leads to the development of a model that shares the ability of both systems. This model was proposed by Jang [19] and was called Adaptive Neuro-Fuzzy Inference System (ANFIS). The ANFIS has adjustable components such as fuzzy rules and membership functions.

The fuzzy rules of a Sugeno fuzzy inference system with two inputs (x and y) and one output (F) are defined as in the following relations:

Rule 1: If (x is A_1) and (y is B_1), then (8)
$F_1=p_1x+q_1y+r_1$

Rule 2: If (x is A_2) and (y is B_2), then (9)
$F_2=p_2x+q_2y+r_2$

in which p_i, q_i, and r_i are adjustable parameters and found using the training procedure. A_i and B_i are fuzzy sets, and F_i is the output of the system. The ANFIS architecture comprises five consecutive layers including fuzzy, product, normalized, defuzzy, and total output layers. The premise and consequent parameters of the ANFIS model were obtained by the training procedure. The consequent and premise parameters of the ANFIS were optimized in two passes. The consequent parameters are calculated by the least square evaluation in forward pass, and the premise parameters are adjusted by the gradient descend in backward [20]. The grid partition technique was employed to determine the optimum configuration of the ANFIS model. The types of the MFs and number of the rules can be chosen through the trial-anderror technique.

According to the flexibility of the ANFIS architecture and parameters, the model can be applied to predict desired values in nonlinear and complicated functions. In this study, the ANFIS model was developed to predict Nu and f in the investigated interrupted plate fins. The CFD modeling was employed to gather further data for training the ANFIS. The CFD-validated-data of the flat and discontinuous fins were applied to train and test the ANFIS models. In the modeling procedure, the Nusselt number and friction factor are the output (target) values; spanwise spacing ratio (p/t), streamwise spacing ratio, (s/r), and Reynolds number (Re) are input parameters. For enhancing the rate of computational process, all input and output data (X_i) were normalized (Y_i) in the range of 0 to 1 as follows:

$$Y_i = \frac{(X_i - X_{min})}{(X_{max} - X_{min})} \quad (10)$$

in which X_{max} and X_{min} are the extreme values of variable X_i.

4. Results and discussion

The experimental setup was provided to study

the four flat and discontinuous fins with various geometric parameters. The fins were modeled using the CFD method, and the modeling results were compared with the experimental data of the investigated fins in Fig. 4. The experimental results were determined at six air frontal velocity, as generated by six-blower rotation speed. The comparison between the experimental and CFD data indicates the validity of the CFD modeling technique. Therefore, the simulation results for more fins with a larger range of the effective variables can be applied as input data of the ANFIS modeling. Fig. 5 shows a comparison between tangential velocity vectors in plain and interrupted plate fins with different geometrical parameters. In the figure, velocity vectors are illustrated in a horizontal slice that goes through a finned surface at H=10 mm. The velocity vectors show that, in the flat and discontinuous fins, the air flow trends to move from a tortuous path. This phenomenon leads to the higher heat transfer coefficients. The change in the geometry of the interrupted plate fin leads to a change in its thermal and flow behaviors. Providing an accurate predictive model for heat transfer rate and pressure drop can be useful in the design of the fined surfaces. As far as the effects of the fin geometries on heat transfer and pressure drop in the fins are quite complicated, two ANFIS models were developed for estimating Nu and f in them.

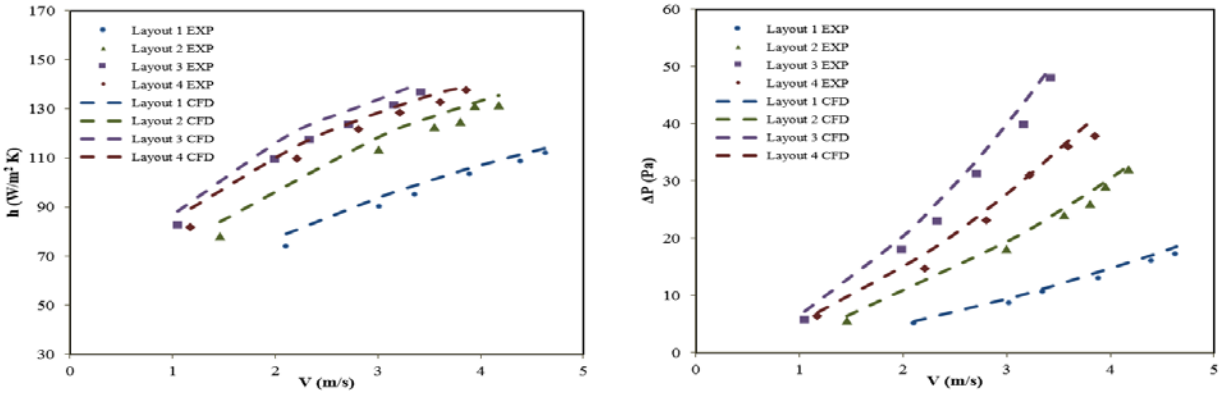

Figure 4. The comparison between experimental and CFD modeling results.

The function of root mean square error (RMSE) was used to find the best ANFIS structure. Moreover, mean relative errors (MRE) function was employed to evaluate the model precision.

The CFD modeling results of the fins with different geometric parameters (reported in Table 2) are used for ANFIS training. A total of 133 numerical-validated data of Nu and f within a Reynolds number ranging from 1117 to 12758 were used for developing the ANFIS. The data points were randomly divided into two subgroups: the first data group (two-third of all of the dataset of Nu and f) was used to train the networks, and the second data group (remaining data) was considered to validate the ANFIS models.

The ANFIS performance by using different membership function (MF) types was investigated. The trial-and-error method was employed to determine the optimum number of rules, as well as types of the MFs in the ANFIS structure. The MFs such as those with forms of triangular, trapezoidal, Generalized

bell, Gaussian, Gaussian mixture, and Π–shaped were examined. The ANFIS with 2, 4, and 4 MFs for the first, second, and third input variables, respectively, has minimum testing RMSE (0.7349). In addition, the application of the combination Gaussian membership function leads to the best prediction result. Input variables were fuzzified using the membership functions, named as MF1 to MF4 in Table 3. The related parameters of the MFs are listed in the table, in which sig1, c1, sig2, and c2 are the combined Gaussian MF parameters [21]. The fuzzy rules of the best first-order Sugeno inference model and optimal consequent parameters for *Nu* modeling are listed in Table 4.

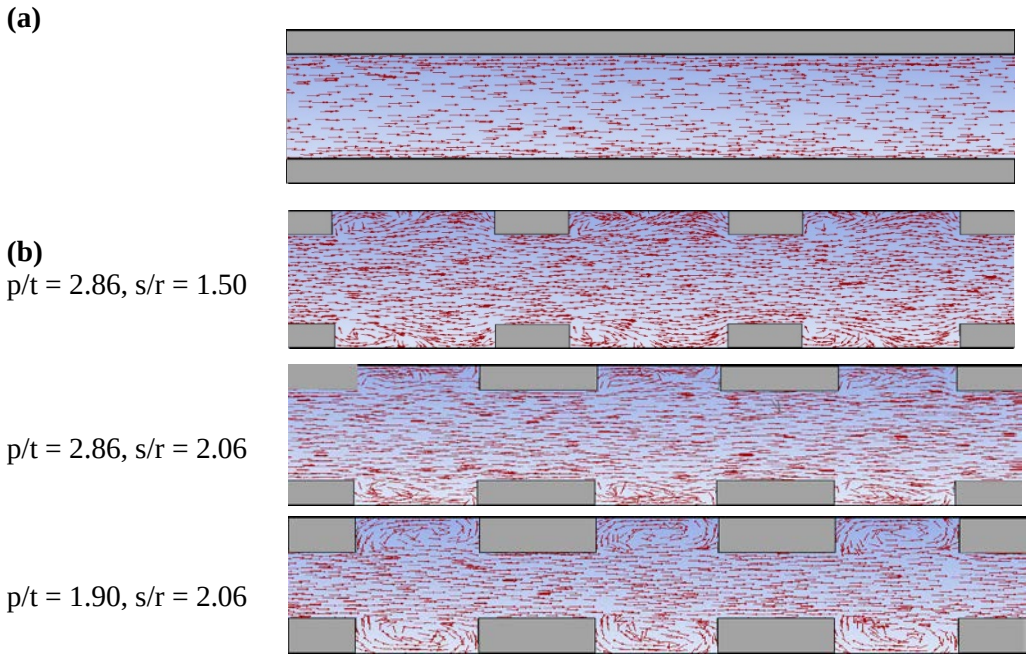

Figure 5. The tangential velocity vectors in top view of (a) plain fin, and (b) interrupted plate fins with different geometries.

Table 3
Parameters of membership functions for *Nu* modeling.

MF function	Parameters	Input 1, *Re*	Input 2, *p/t*	Input 3, *s/r*
MF1	sig1	0.1699	0.05662	0.05662
	c1	-0.3	-0.1	-0.1
	sig2	0.1956	0.04903	0.1327
	c2	0.1075	0.02513	0.152
MF2	sig1	0.1466	0.07827	0.05685
	c1	0.4704	0.1803	0.2333
	sig2	0.1699	0.04282	0.05613
	c2	1.3	0.4278	0.4309
MF3	sig1	-	0.1055	0.07819
	c1	-	0.5293	0.5477
	sig2	-	0.04863	0.05194
	c2	-	0.7563	0.7654
MF4	sig1	-	0.0775	0.05671
	c1	-	0.885	0.9
	sig2	-	0.0566	0.05662
	c2	-	1.1	1.1

Table 4
Fuzzy rules of the optimum ANFIS structure for prediction of *Nu*.

Rule number	Rule description
1	If (Re is Re MF1) and (p/t is p/t MF1) and (s/r is s/r MF1) then (Nu=0.818×Re-0.01115×p/t-0.00464×s/r-0.02114)
2	If (Re is Re MF1) and (p/t is p/t MF1) and (s/r is s/r MF2) then (Nu=-0.1001×Re-0.128×p/t+0.03762×s/r+0.06507)
3	If (Re is Re MF1) and (p/t is p/t MF1) and (s/r is s/r MF3) then (Nu=0.7896×Re-0.0551×p/t+0.03079×s/r+0.06413)
4	If (Re is Re MF1) and (p/t is p/t MF1) and (s/r is s/r MF4) then (Nu=0.08731×Re-0.001858×p/t-0.03901s/r-0.04057)
5	If (Re is Re MF1) and (p/t is p/t MF2) and (s/r is s/r MF1) then (Nu=0.484×Re+0.001426×p/t+0.1463×s/r-0.001394)
6	If (Re is Re MF1) and (p/t is p/t MF2) and (s/r is s/r MF2) then (Nu=0.5535×Re+0.342×p/t-0.1198×s/r+0.1114)
7	If (Re is Re MF1) and (p/t is p/t MF2) and (s/r is s/r MF3) then (Nu=0.5205×Re+0.2158×p/t+0.1407×s/r+0.06005)
8	If (Re is Re MF1) and (p/t is p/t MF2) and (s/r is s/r MF4) then (Nu=0.4588×Re-0.5285×p/t-0.6256×s/r+0.9781)
9	If (Re is Re MF1) and (p/t is p/t MF3) and (s/r is s/r MF1) then (Nu=0.5747×Re+0.05059×p/t+0.02955×s/r+0.09005)
10	If (Re is Re MF1) and (p/t is p/t MF3) and (s/r is s/r MF2) then (Nu=0.9806×Re+0.0473×p/t+0.02884×s/r+0.13)
11	If (Re is Re MF1) and (p/t is p/t MF3) and (s/r is s/r MF3) then (Nu=0.3688×Re+0.0968×p/t+0.1105×s/r+0.1608)
12	If (Re is Re MF1) and (p/t is p/t MF3) and (s/r is s/r MF4) then (Nu=0.3549×Re+0.1937×p/t+0.2685×s/r+0.1361)
13	If (Re is Re MF1) and (p/t is p/t MF4) and (s/r is s/r MF1) then (Nu=0.0001031×Re-8.311×10^{-6}×p/t+4.472×10^{-6}×s/r-3.2×10^{-5})
14	If (Re is Re MF1) and (p/t is p/t MF4) and (s/r is s/r MF2) then (Nu=-0.009956×Re-0.0009904×p/t-0.0006617×s/r-0.001507)
15	If (Re is Re MF1) and (p/t is p/t MF4) and (s/r is s/r MF3) then (Nu=1.228×Re+0.09175×p/t+0.07441×s/r+0.1142)
16	If (Re is Re MF1) and (p/t is p/t MF4) and (s/r is s/r MF4) then (Nu=0.3188×Re+0.1478×p/t+0.1416×s/r+0.1478)
17	If (Re is Re MF2) and (p/t is p/t MF1) and (s/r is s/r MF1) then (Nu=0.7022×Re-0.01512×p/t-0.0343×s/r-0.1307)
18	If (Re is Re MF2) and (p/t is p/t MF1) and (s/r is s/r MF2) then (Nu=0.1895×Re-0.1734×p/t+0.06919×s/r+0.05741)
19	If (Re is Re MF2) and (p/t is p/t MF1) and (s/r is s/r MF3) then (Nu=0.6297×Re-0.08706×p/t-0.04673×s/r-0.02421)
20	If (Re is Re MF2) and (p/t is p/t MF1) and (s/r is s/r MF4) then (Nu=0.2606×Re-0.02497×p/t-0.2885×s/r+0.3006)
21	If (Re is Re MF2) and (p/t is p/t MF2) and (s/r is s/r MF1) then (Nu=0.7866×Re-0.03845×p/t+0.196×s/r-0.1827)
22	If (Re is Re MF2) and (p/t is p/t MF2) and (s/r is s/r MF2) then (Nu=0.2758×Re+0.4734×p/t-0.1628×s/r+0.1445)
23	If (Re is Re MF2) and (p/t is p/t MF2) and (s/r is s/r MF3) then (Nu=0.2894×Re+0.3307×p/t+0.2093×s/r+0.07956)
24	If (Re is Re MF2) and (p/t is p/t MF2) and (s/r is s/r MF4) then (Nu=0.2863×Re-1.809×p/t-2.175×s/r+2.898)
25	If (Re is Re MF2) and (p/t is p/t MF3) and (s/r is s/r MF1) then (Nu=0.9266×Re+0.05009×p/t+0.03099×s/r+0.08608)
26	If (Re is Re MF2) and (p/t is p/t MF3) and (s/r is s/r MF2) then

	(Nu=0.2777×Re+0.05337×p/t+0.03735×s/r+0.1507)
	If (Re is Re MF2) and (p/t is p/t MF3) and (s/r is s/r MF3) then
27	(Nu=0.7074×Re+0.1539×p/t+0.1743×s/r+0.2602)
	If (Re is Re MF2) and (p/t is p/t MF3) and (s/r is s/r MF4) then
28	(Nu=0.4573×Re+0.4612×p/t+0.4969×s/r+0.6323)
	If (Re is Re MF2) and (p/t is p/t MF4) and (s/r is s/r MF1) then
29	(Nu=0.000535×Re+2.582×10^{-5}×p/t+3.2×10^{-5}×s/r+1.08×10^{-5})
	If (Re is Re MF2) and (p/t is p/t MF4) and (s/r is s/r MF2) then
30	(Nu=0.003544×Re-0.0009628×p/t-0.0006406×s/r-0.001471)
	If (Re is Re MF2) and (p/t is p/t MF4) and (s/r is s/r MF3) then
31	(Nu=0.1135×Re+0.1301×p/t+0.1055×s/r+0.162)
	If (Re is Re MF2) and (p/t is p/t MF4) and (s/r is s/r MF4) then
32	(Nu=0.356×Re+0.2209×p/t+0.2117×s/r+0.2209)

Moreover, the ANFIS with a structure of 2/2/2 and 8 fuzzy rules leads to the lowest RMSE for predicting *f* on the investigated fined surfaces. The results show that the models with more MFs and fuzzy rules resulted in complex networks and lower prediction accuracy. The selected model configuration has trapezoidal MFs. Table 5 reports the parameters of the input fuzzy sets in which a, b, and c are the trapezoidal MF parameters [21]. The 8 fuzzy rules of the ANFIS, developed for predicting the friction factor, are listed in Table 6.

Table 5
Parameters of the membership functions for *f* modeling.

Membership function	Parameters	Input 1, *Re*	Input 2, *p/t*	Input 3, *s/r*
MF1	a	-1	-1	-1
	b	-0.02003	-0.009301	-0.007811
	c	1.017	1.009	1.02
MF2	a	0.04807	0.04092	0.06756
	b	0.9794	0.9903	0.9791
	c	2	2	2

Table 6
Fuzzy rules of the optimum ANFIS structure for predicting *f*.

Rule number	Rule description
	If (Re is Re MF1) and (p/t is p/t MF1) and (s/r is s/r MF1) then
1	(Nu=-0.4072×Re-9.039×p/t+1.444×s/r+0.5582)
	If (Re is Re MF1) and (p/t is p/t MF1) and (s/r is s/r MF2) then
2	(Nu=-11.67×Re+1.379×p/t+1.384×s/r+0.281)
	If (Re is Re MF1) and (p/t is p/t MF2) and (s/r is s/r MF1) then
3	(Nu=-4.985×Re-8.665×p/t+1.22×s/r+8.646)
	If (Re is Re MF1) and (p/t is p/t MF2) and (s/r is s/r MF2) then
4	(Nu=-6.734×Re+1.532×p/t-0.1737×s/r-0.1776)
	If (Re is Re MF2) and (p/t is p/t MF1) and (s/r is s/r MF1) then
5	(Nu=0.5216×Re-6.137×p/t-5.241×s/r+0.2273)
	If (Re is Re MF2) and (p/t is p/t MF1) and (s/r is s/r MF2) then
6	(Nu=-10.04×Re-1.353×p/t-5.173×s/r+16.35)
	If (Re is Re MF2) and (p/t is p/t MF2) and (s/r is s/r MF1) then
7	(Nu=-2.237×Re-4.349×p/t-0.5319×s/r+8.623)
	If (Re is Re MF2) and (p/t is p/t MF2) and (s/r is s/r MF2) then
8	(Nu=-5.768×Re-1.025×p/t+0.5234×s/r+6.737)

Fig. 6 indicates the comparison between the numerical-validated values obtained from CFD modeling and the predicted results from the developed ANFIS models. The solid line shows the perfect fit (predicted equal target value). The figure illustrates that the ANFIS-predicted values for all data points are quite close to the CFD-validated data. The investigated data are in testing data set for *Nu* and *f* modeling. The calculated MRE values of 1.33 % and 3.32 % for prediction of *Nu* and *f*, respectively, indicate the validation of the neuro-fuzzy models.

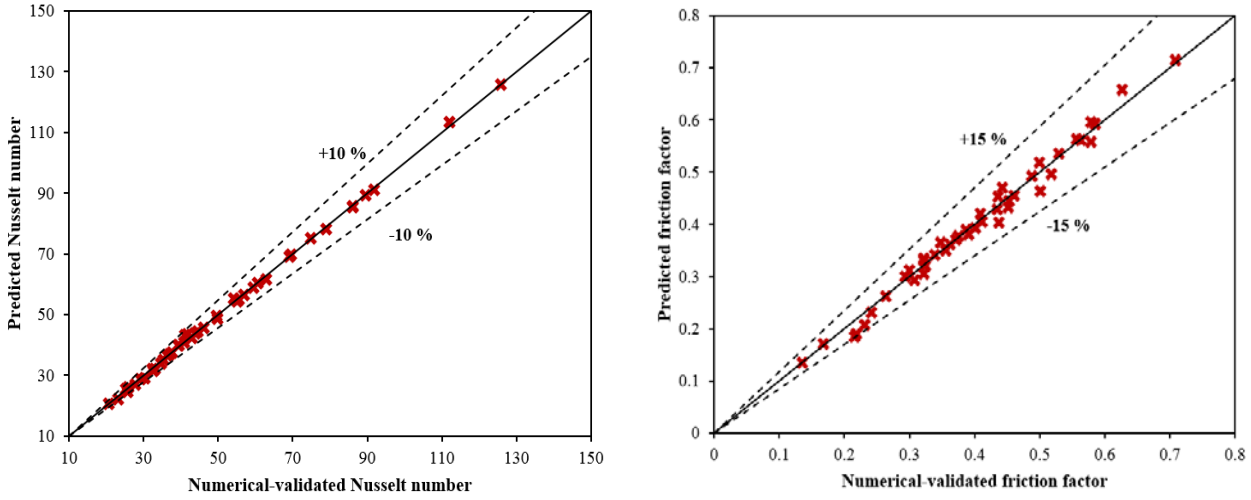

Figure 6. The evaluation of the ANFIS accuracy for prediction of (a) Nusselt number and (b) friction factor.

5. Conclusions

This study attempted to introduce the precision of Adaptive Neuro-Fuzzy Inference System (ANFIS) for evaluating the thermal and friction characteristics of air convection on flat and discontinuous fins. For avoiding experimental effort, the numerical-validated data obtained from the CFD modeling were used for training the ANFIS. Two Neuro-Fuzzy models were proposed to estimate Nu and f as functions of spanwise spacing ratio, streamwise spacing ratio, and Reynolds number. The grid partition method was used for developing the ANFIS structure. The high precision of the models for prediction of the test data group (which was not introduced to the ANFIS before training) indicates the validity of the techniques.

Nomenclature

A_{tot}	total heat transfer area [m^2].
b	height of the base plate [m].
C_p	specific heat capacity [kJ/kg K].
D_h	hydraulic diameter [m].
h	heat transfer coefficient [W/m^2 K].
H	fin height [m].
f	friction factor.
k	thermal conductivity [W/m K].
L	length of the finned surface [m].
Nu	Nusselt number.
p	fin pitch [m].
Q	heat transfer rate [W].
Re	Reynolds number.
r	fin length [m].
s	fin interruption [m].
T	temperature [K].
t	fin thickness [m].
ΔP	pressure drop [Pa].
u	velocity [m/s].

W	width of the finned surface [m].
Greek letters	
μ	dynamic viscosity [Pa s].
ρ	density [kg/m^3].
Subscripts	
In	inlet.
lm	logarithmic mean.
min	minimum.
max	maximum.
Out	outlet.

References

[1] Vasudevan, R., Eswaran, V. and Biswas, G., "Winglet-type vortex generators for plate-fin heat exchangers using triangular fins", *Numer. Heat Tr. A-Appl.*, **38**, 533 (2000).

[2] Diani, A., Mancin, S., Zilio, C. and Rossetto, L., "An assessment on air forced convection on extended surfaces: Experimental results and numerical modeling", *Int. J. Therm. Sci.*, **67**, 120 (2013).

[3] Yazicioğlu, B. and Yüncü, H., "Optimum fin spacing of rectangular fins on a vertical base in free convection heat transfer", *Heat Mass Transf.*, **44**, 11 (2007).

[4] Rao, Y., Xu, Y. and Wan, C., "An experimental and numerical study of flow and heat transfer in channels with pin fin-dimple and pin fin arrays", *Exp. Therm. Fluid Sci.*, **38**, 237 (2012).

[5] Guan, X., Gao, Y., Tian, Z., Wang, L., Cheng, Y. and Li, X., "Hydrodynamics in bubble columns with pin-fin tube internals", *Chem. Eng. Res. Des.*, **102**, 196 (2015).

[6] Zhao, J., Huang, S., Gong, L. and Huang, Z., "Numerical study and optimizing on micro square pin-fin heat sink for electronic cooling", *Appl. Therm. Eng.*, **93**, 1347 (2016).

[7] Bhowmik, H. and Lee, K. S., "Analysis of heat transfer and pressure drop characteristics in an offset strip fin heat exchanger", *Int. Commun. Heat Mass*, **36**, 259 (2009).

[8] Yujie, Y., Yanzhong, L., Biao, S. and Jieyu, Z., "Performance evaluation of heat transfer enhancement in plate-fin heat exchangers with offset strip fins", *Phys. Procedia*, **67**, 543 (2015).

[9] Priyam, A. and Chand, P., "Thermal and thermohydraulic performance of wavy finned absorber solar air heater", *Sol. Energy*, **103**, 250 (2016).

[10] Du, X., Feng, L., Li, L., Yang, L. and Yang, Y., "Heat transfer enhancement of wavy finned flat tube by punched longitudinal vortex generators", *Int. J. Heat Mass Tran.*, **75**, 368 (2014).

[11] Khoshvaght-Aliabadi, M., Hormozi, F. and Zamzamian, A., "Role of channel shape on performance of plate-fin heat exchangers: Experimental assessment", *Int. J. Therm. Sci.*, **79**, 183 (2014).

[12] Mon, M. S. and Gross, U., "Numerical study of fin-spacing effects in annular-finned tube heat exchangers", *Int. J. Heat Mass Tran.*, **47**, 1953 (2004).

[13] Bar, N., Bandyopadhyay, T. K., Biswas, M. N. and Das, S. K., "Prediction of pressure dropusing artificial neural network for non-Newtonian liquid flow through piping components", *J. Petrol. Sci. Eng.*, **71**, 187 (2010).

[14] Rahimi, M., Hajialyani, M., Beigzadeh, R. and Alsairafi, A. A., "Application of artificial neural network and genetic algorithm approaches for prediction of flow characteristic in serpentine microchannels", *Chem. Eng. Res. Des.*, **98**, 147 (2015).

[15] Momayez, L., Dupont, P., Delacourt, G., Lottin, O. and Peerhossaini, H., "Genetic algorithm based correlations for heat transfer calculation on concave surfaces", *Appl. Therm. Eng.*, **29**, 3476 (2009).

[16] Holman, J. P., Experimental methods for engineers, 3rd ed., McGraw-Hill, New York, (2011).

[17] Launder, B. E. and Spalding, D., "The numerical computation of turbulent flows", *Comput. Method Appl. M.*, **3**, 269 (1974).

[18] Wieland, D., Wotawa, F. and Wotawa, G., "From neural networks to qualitative models in environmental engineering", *Comput-Aided Civ. Inf.*, **17**, 104 (2002).

[19] Jang, J. S. R., "ANFIS: adaptive-network-based fuzzy inference system", *IEEE Trans. Syst. Man. Cybern.*, **23**, 665 (1993).

[20] Atmaca, H., Cetisli, B. and Yavuz, H. S., "The comparison of fuzzy inference systems and neural network approaches with ANFIS method for fuel consumption data", Proceeding of *Second International Conference on Electrical and Electronics Engineering Papers ELECO'2001*, Bursa, Turkey, (2001).

[21] The MathWorks Inc., www.mathworks.com.